Supplementary Figure 1

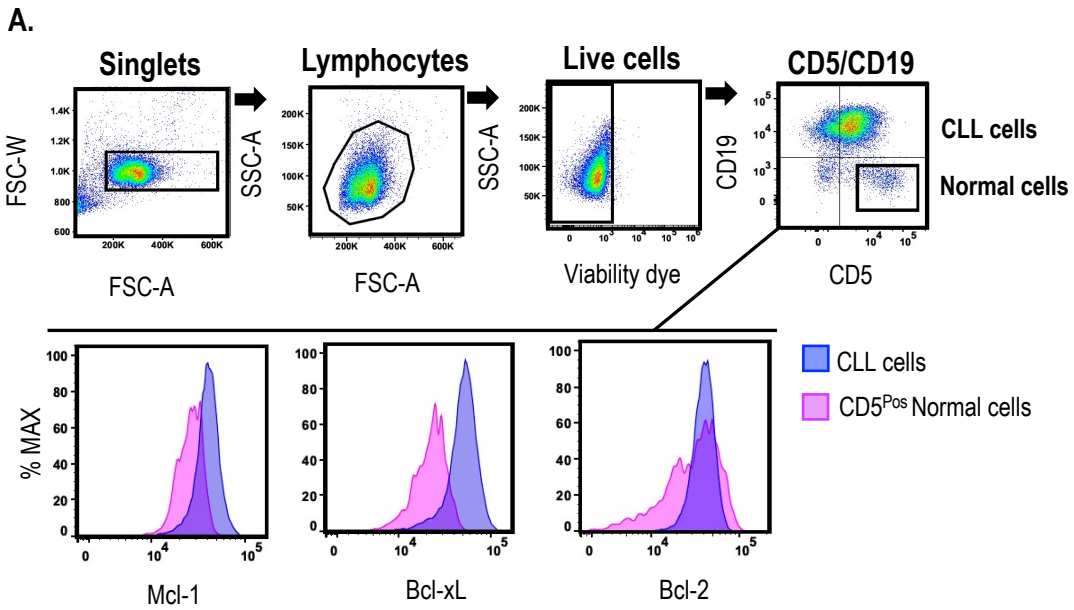

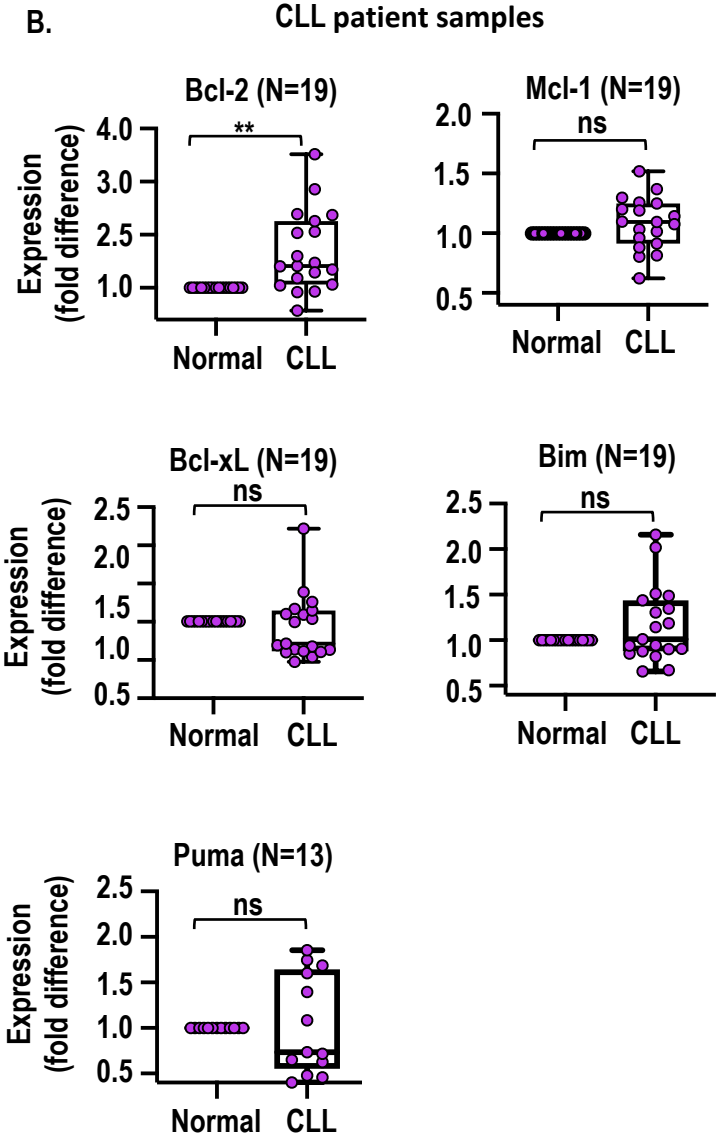

Supplementary Figure 2

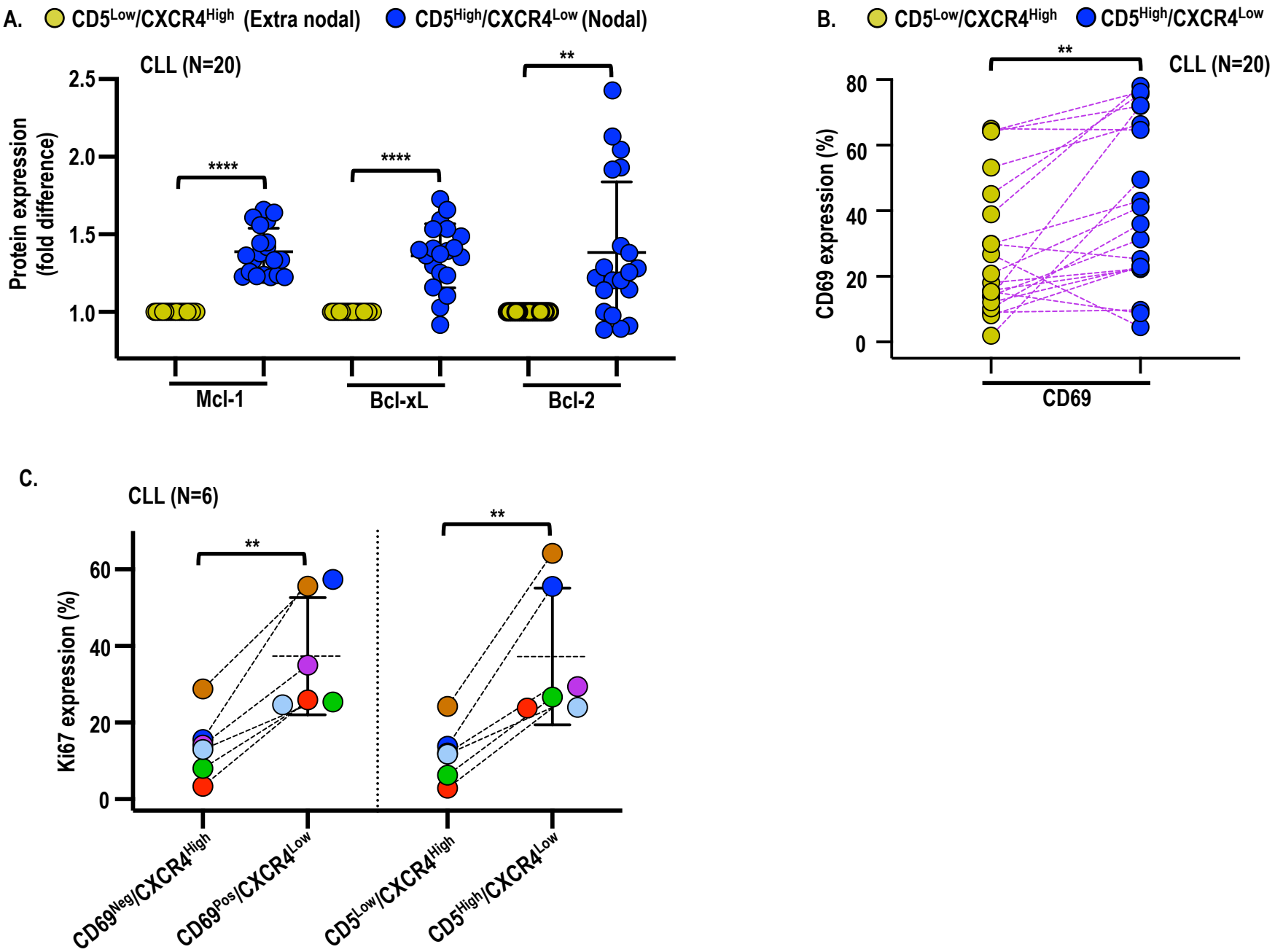

Supplementary Figure 3

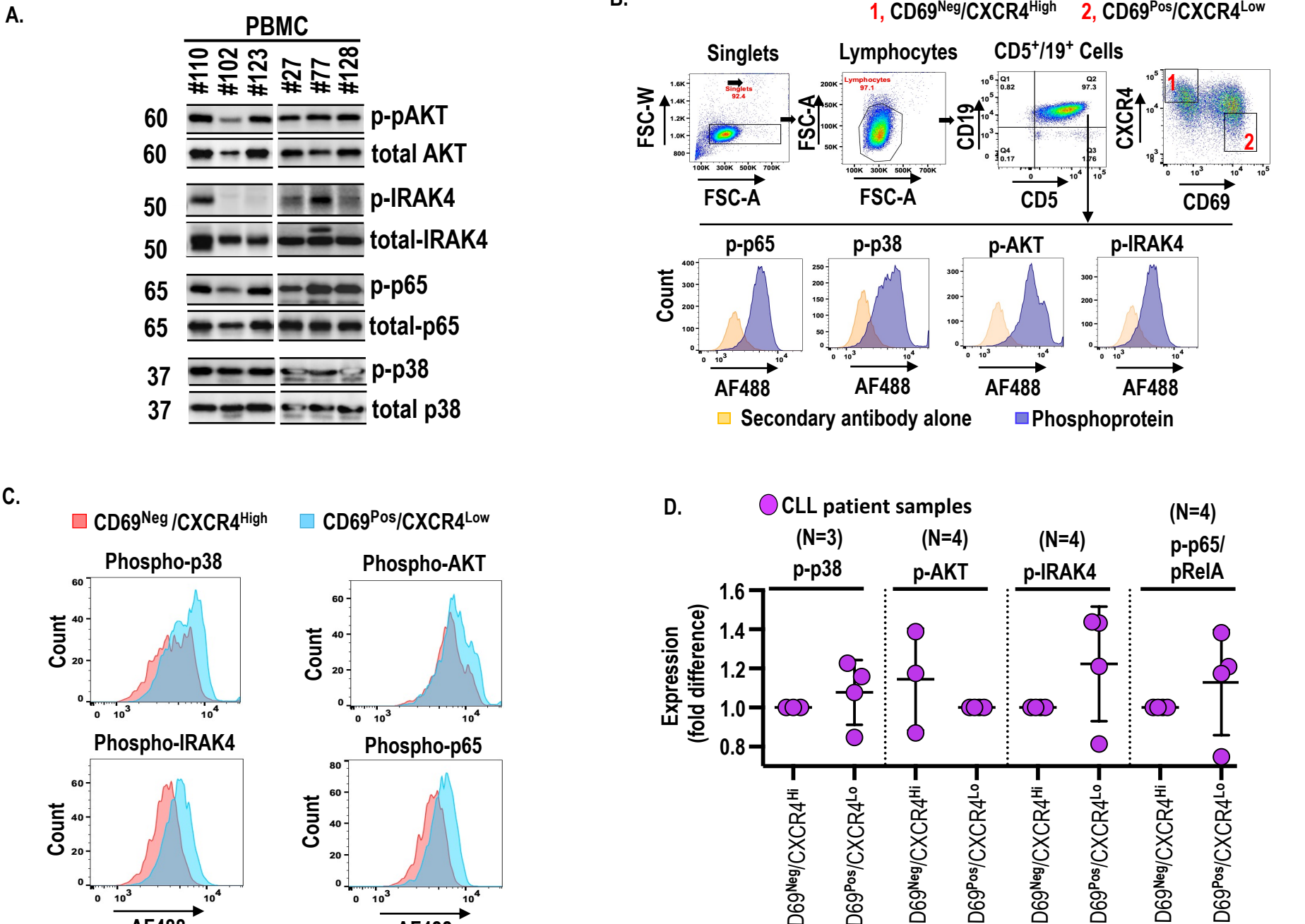

Supplementary Figure 4

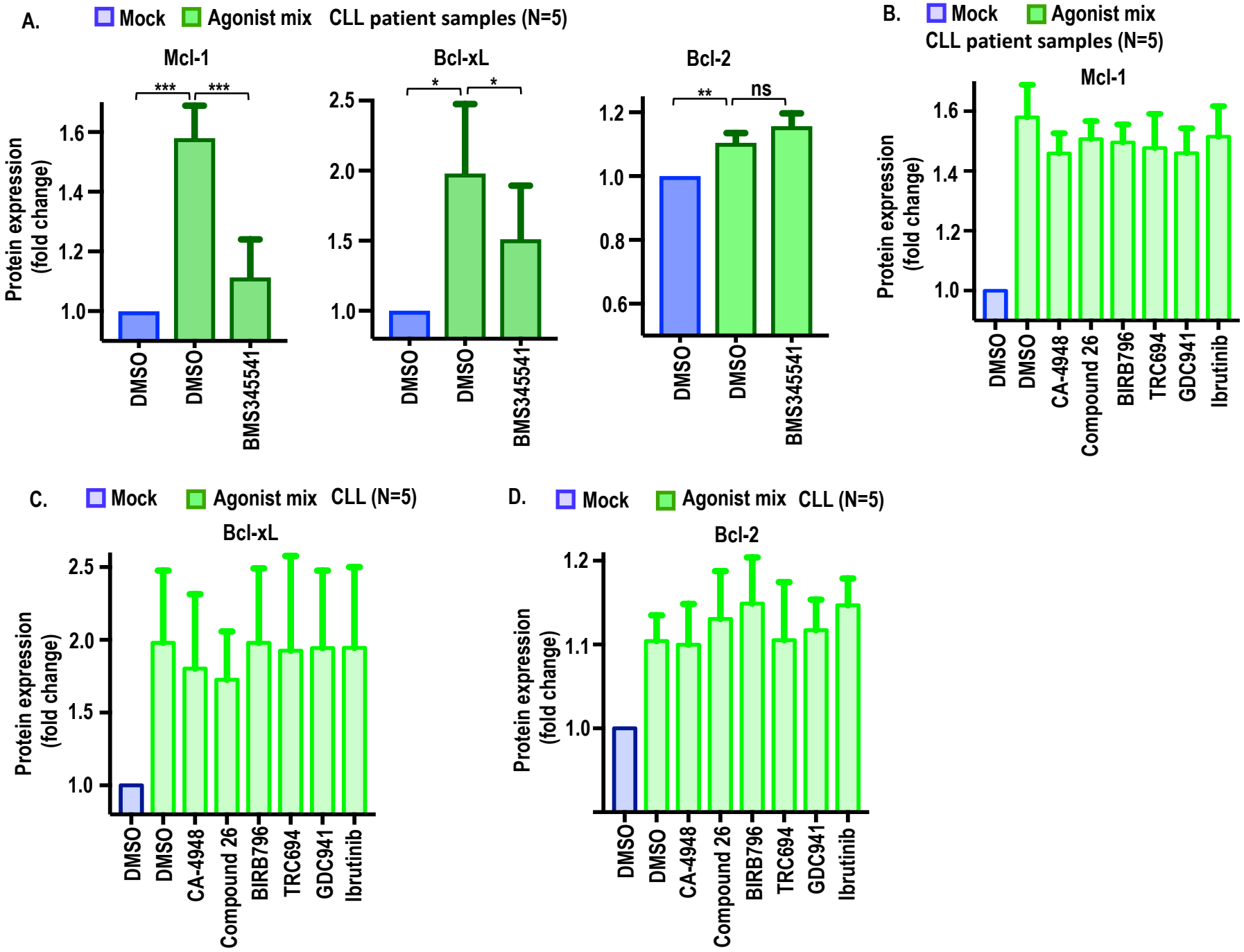

Supplementary Figure 5

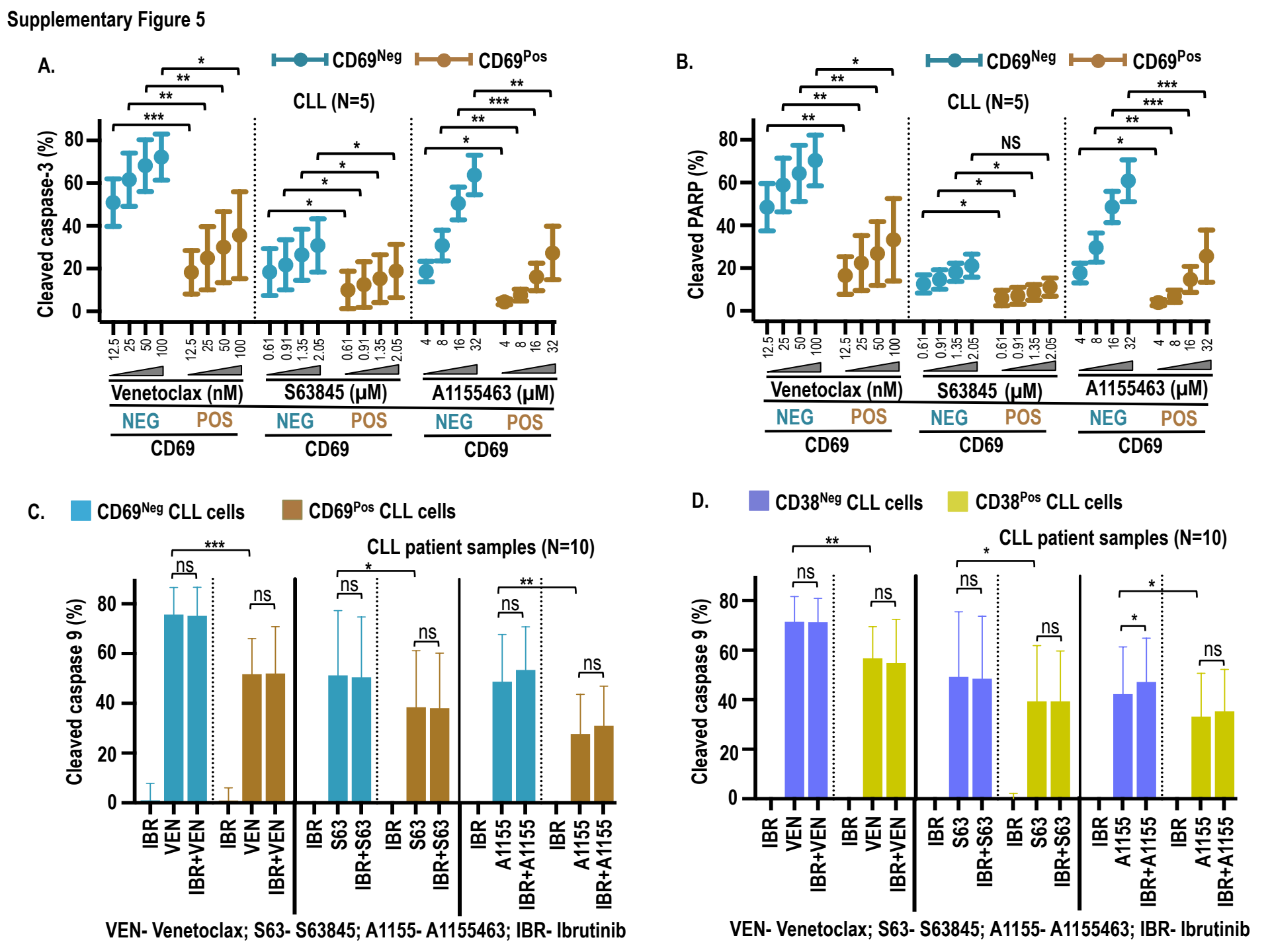

Supplementary Figure 5

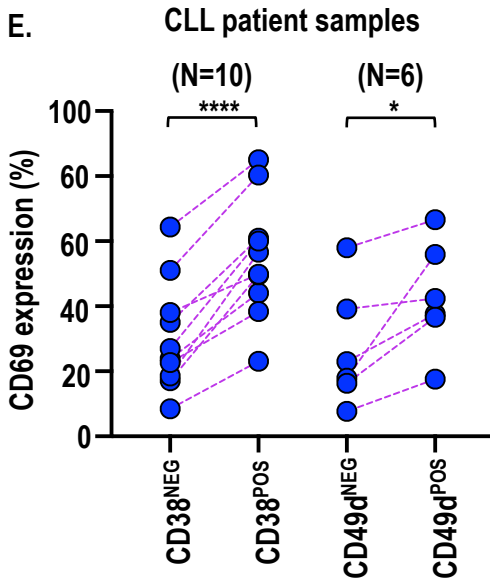

Supplementary Figure 6

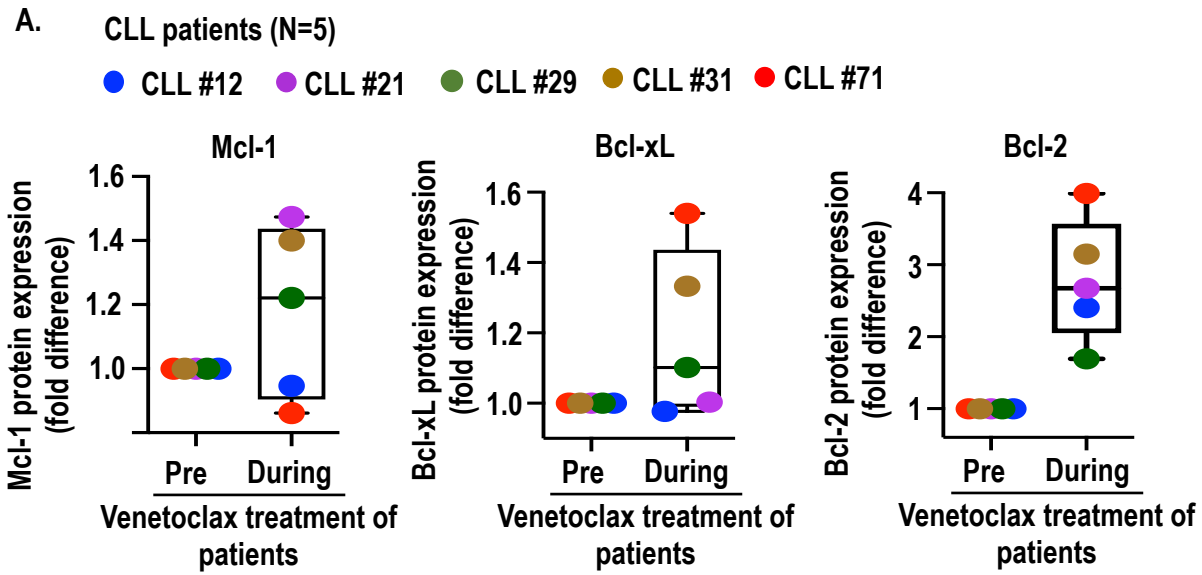

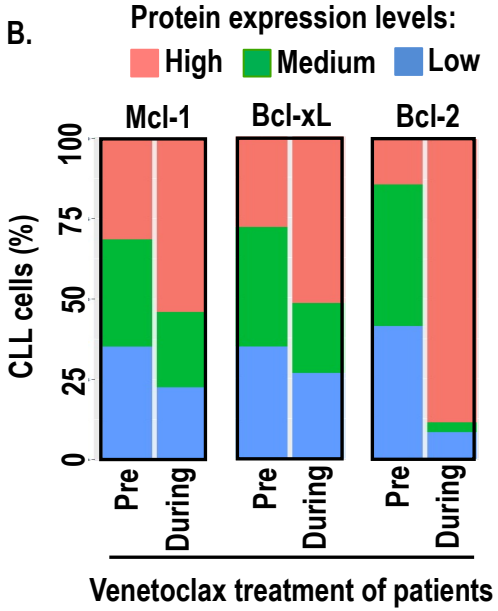

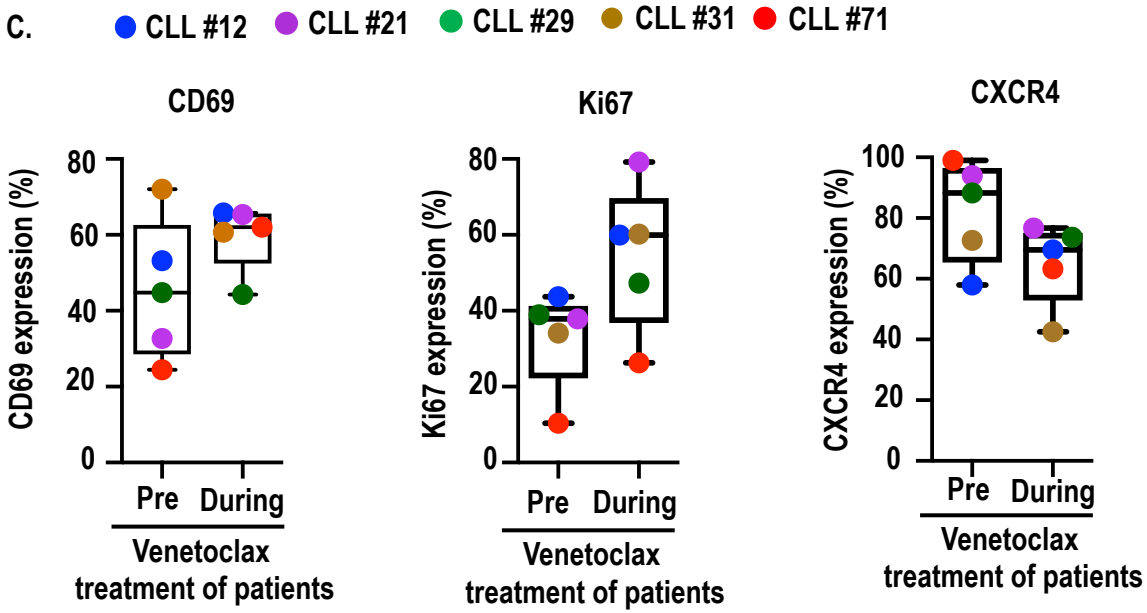

Supplementary Figure 7

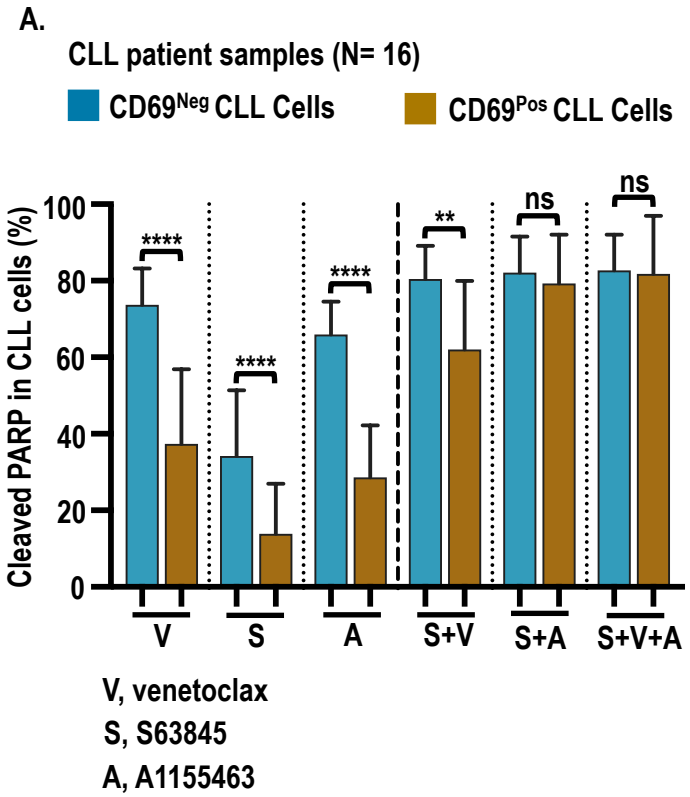

V, venetoclax
S, S63845
A, A1155463

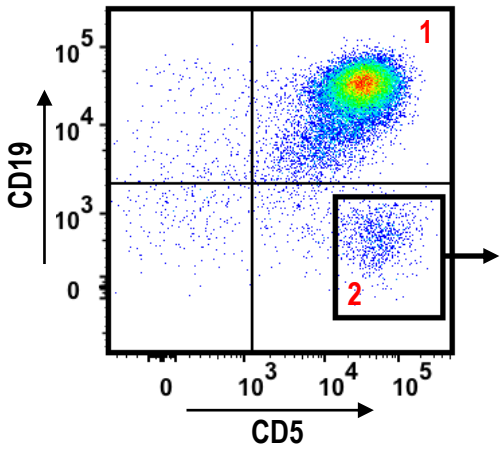

1, CLL cells

2, Non-leukemic lymphocytes

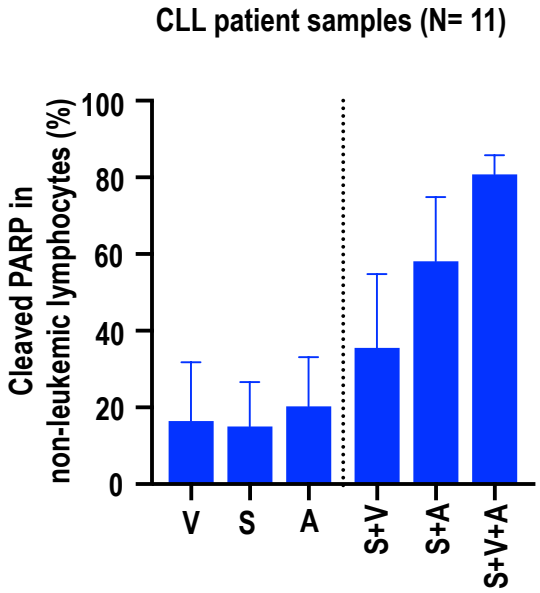

Supplementary Figure 8

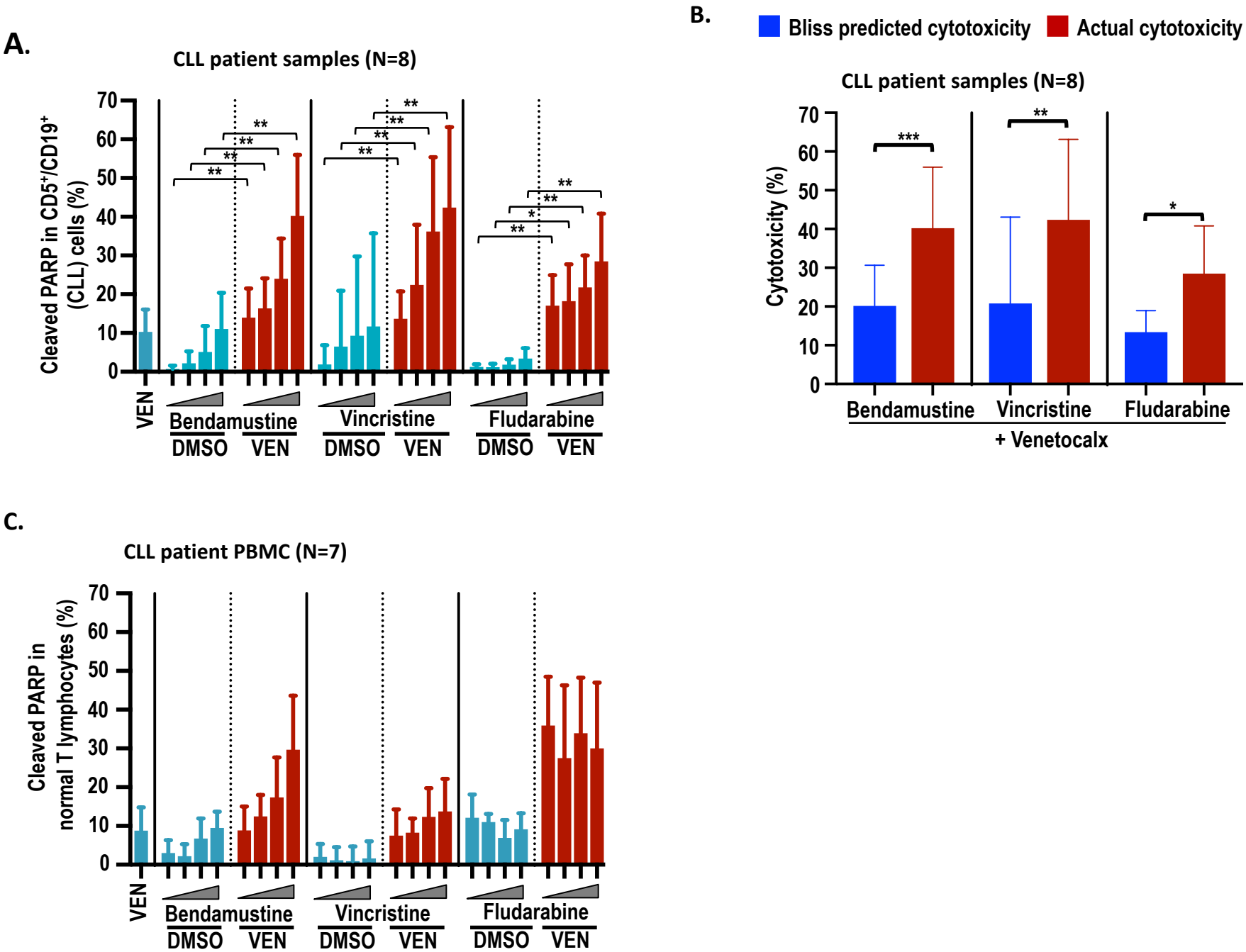

Supplementary Figure 9

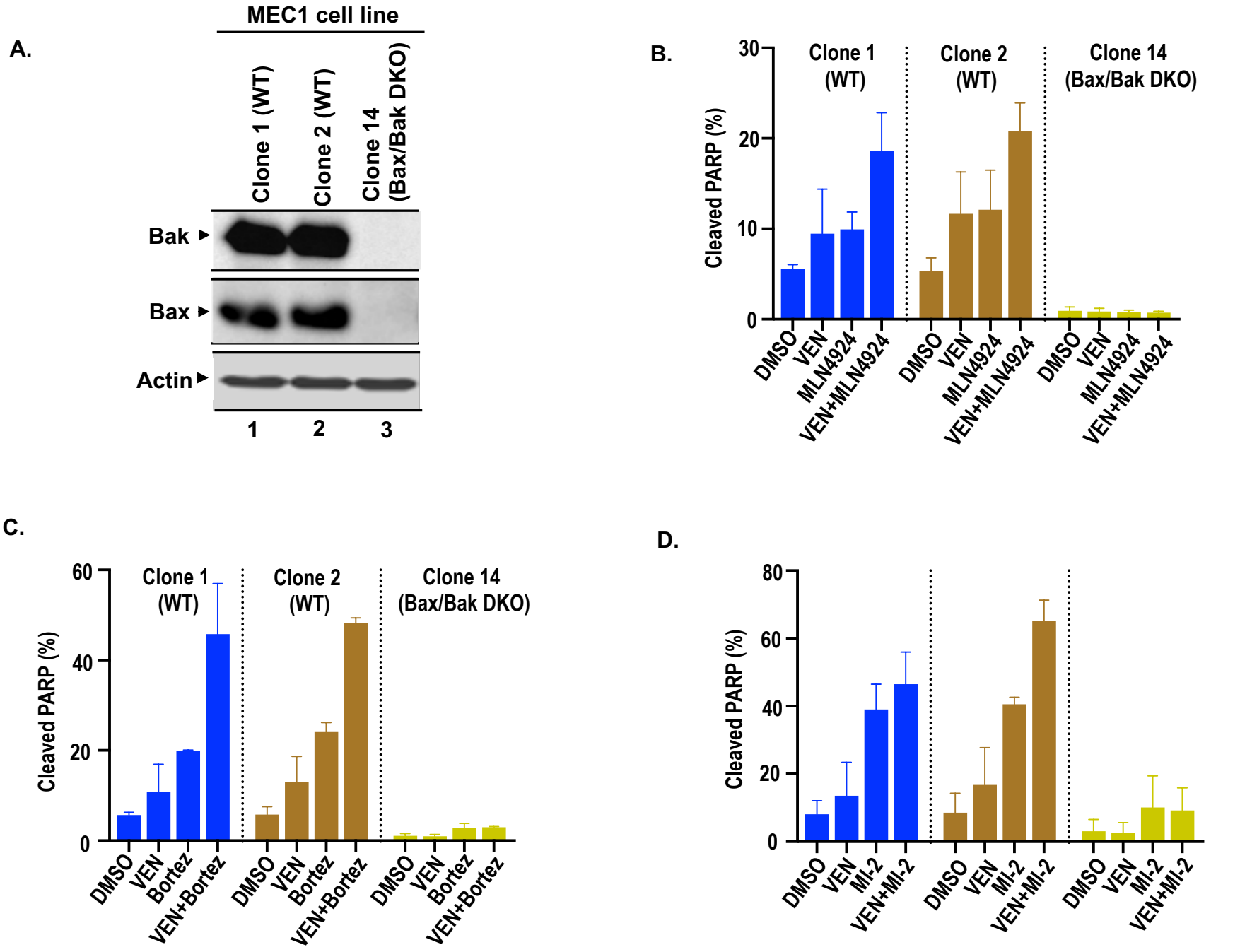

Supplementary Figure 10

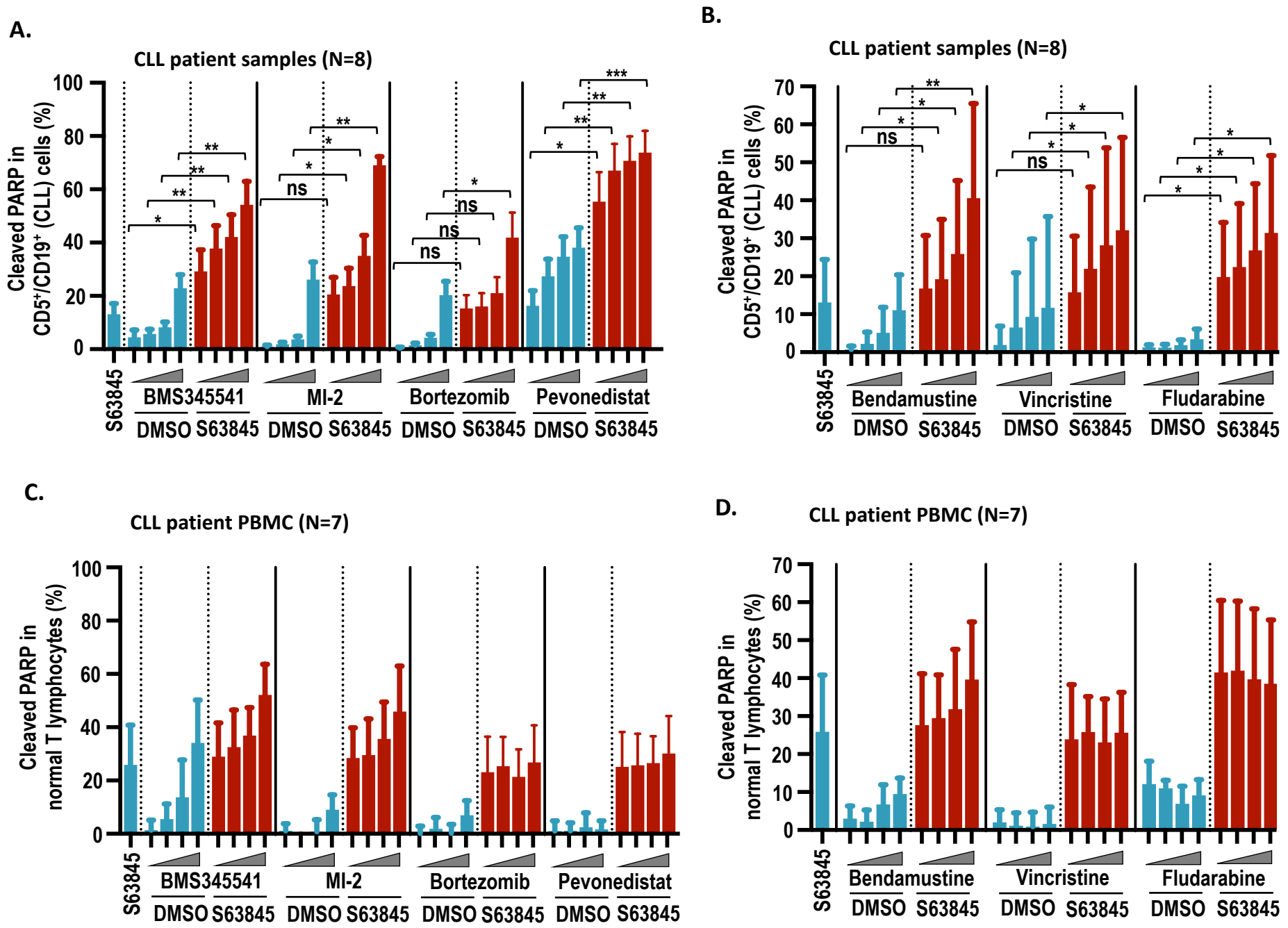

Supplementary Figure 11

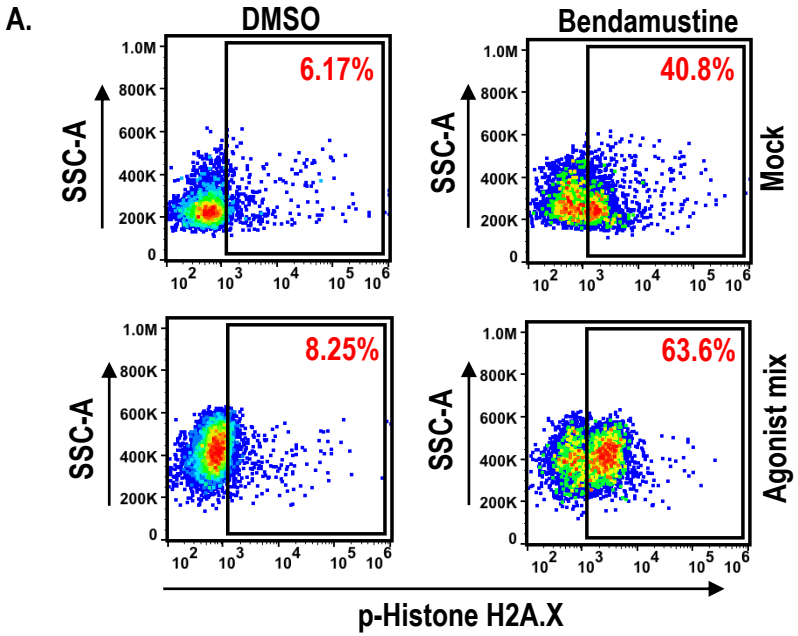

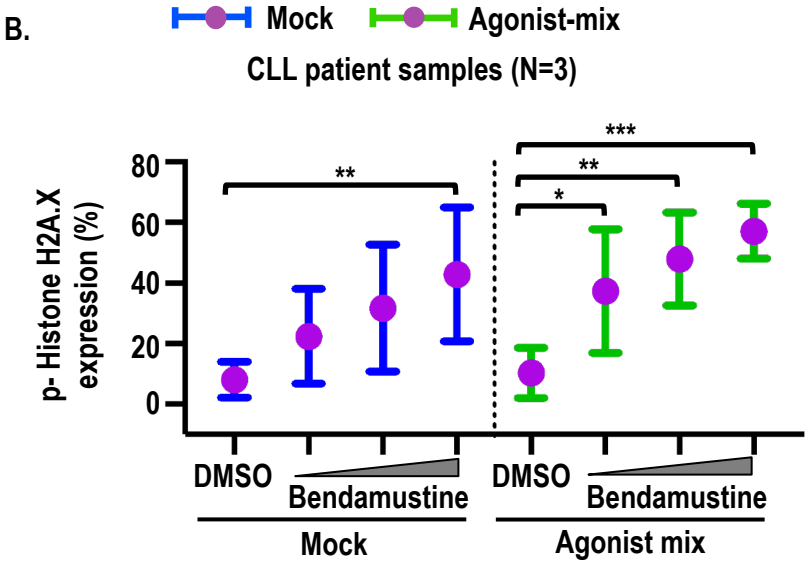

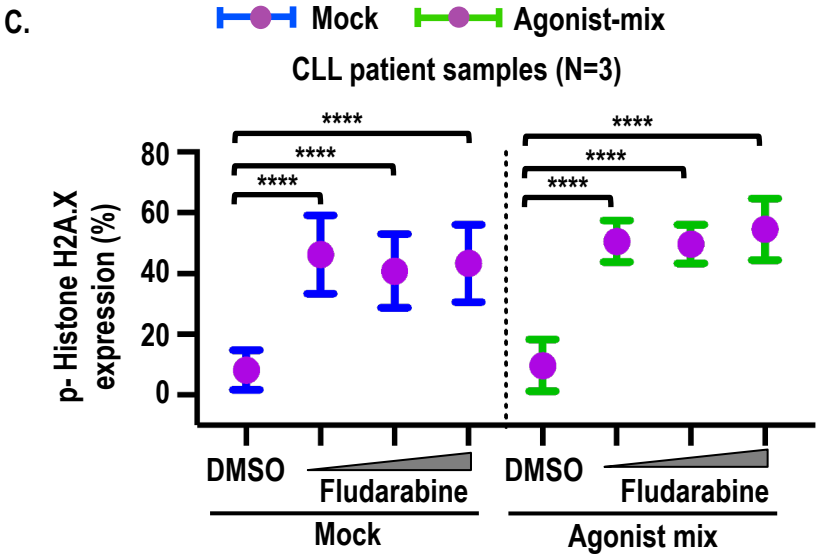

Supplementary figure legends.

Supplementary Figure 1. The patient sample profiling reveals overexpression of Bcl-2 in CLL cells as compared to healthy lymphocytes in patient PBMC. (A-B) The expression of apoptotic proteins Mcl-1, Bcl-xL, Bcl-2, Bim, Puma, Bak, and Bax was analyzed by FCM using freshly frozen CLL patient PBMCs (N=18). **(A)** The FCM gating strategy showing identification of CLL ($CD5^{+}/CD19^{+}$) and CD5 positive non-leukemic lymphocytes and expression of Mcl-1, Bcl-xL, and Bcl-2 in CLL and non-leukemic lymphocytes in a representative patient PBMC sample. We were unable to assess apoptotic protein expression in healthy B ($CD19+/CD5^{-}$) cells, since these cells were not readily detectable as a distinct population in most patients. **(B)** The expression of apoptotic proteins in CLL and CD5 positive non-leukemic lymphocytes analyzed from multiple CLL patients (N=17). The data is presented as fold difference in geometric mean fluorescence intensity (GMFLI) in CLL **(**viability $dye^{Neg}/CD5^{+}/CD19^{+}$) cells as compared to non-leukemic lymphocytes **(**viability $dye^{Neg}/CD5^{+}/CD19^{-}$). Statistical significance was determined by Student *t*-test. *p<0.05, **p<0.01, ns- not significant. Data is presented as mean ± SD. Statistical significance was determined by ANOVA with Sidak's post-hoc test for multiple comparisons. *p<0.05. Data is presented as mean ± SD.

Supplementary Figure 2. Circulating leukemic B-cells recently emigrated from the lymph node in CLL patients are enriched for cells overexpressing multiple anti-apoptotic proteins. (A) Patient PBMCs (N=20) were examined using FCM for expression of apoptotic proteins as described in Figure 1A-B. Data showing fold difference in geometric mean fluorescence intensity (GMFLI) of anti-apoptotic proteins Mcl-1, Bcl-xL, and Bcl-2 in $CD5^{High}/CXCR4^{Low}$ (nodal) as compared to $CD5^{Low}/CXCR4^{High}$ (extra nodal) CLL cells. **(B)** Data showing percentage CD69 positive cells in $CD5^{High}/CXCR4^{Low}$ (nodal) and $CD5^{Low}/CXCR4^{High}$ (extra nodal) CLL cells. **(C)** Data showing percentage Ki67 positive cells in $CD5^{High}/CXCR4^{Low}$ (nodal) and $CD5^{Low}/CXCR4^{High}$ (extra nodal) CLL cells as well as $CD69^{Pos}/CXCR4^{Low}$ (nodal) and $CD69^{Neg}/CXCR4^{High}$ (extra nodal) CLL cells. Data is presented as mean ± SD. Statistical significance was determined by ANOVA with Sidak's post-hoc test for multiple comparisons. **p<0.01, ****p<0.0001. Data is presented as mean ± SD.

Supplementary Figure 3. CLL cells with CD69^{Pos} activation phenotype *in vivo* exhibit upregulation of multiple signaling pathways with substantial inter-patient variability. (A) PBMCs containing over 90% leukemic B-cells were isolated from fresh blood of CLL patients in presence of pervanadate and calyculin A using SepMate kit. Expression of total and p-p65, p-p38, p-AKT, or p-IRAK4 was analyzed by Western blot (WB) using corresponding antibodies. (**B-D)** PBMCs were isolated from fresh blood of CLL patients as described in panel A and stained for phosphoproteins, as described in Supplementary Methods. (B) FCM gating strategy showing analysis of phosphoproteins in CD69$^{Pos/Neg}$/CXCR4$^{Low/High}$ CLL **(**CD5^{+}/CD19^{+}) cells in patient PBMCs. (C) Representative flow histograms showing expression of p-IRAK4, p-AKT, p-p38, and p-p65 in CD69^{Neg}/CXCR4^{High} and CD69^{Pos}/CXCR4^{Low} CLL (CD5^{+}/CD19^{+}) cells in PBMC isolated from fresh blood of a CLL patient (Pt 33). (D) Data showing fold difference in geometric mean fluorescence intensity (GMFLI) of p-IRAK4, p-AKT, p-p38, and p-p65 in CD69^{Pos}/CXCR4^{Low} CLL (CD5^{+}/CD19^{+}) cells as compared to CD69^{Neg}/CXCR4^{High} CLL cells in multiple patients. Data is presented as mean ± SD.

Supplementary Figure 4. Inhibition of NF-kB signaling but not AKT, BTK, IRAK4, or p38 blocks the upregulation of anti-apoptotic proteins in microenvironmentally-activated CLL cells. (A) CLL patient PBMC (N=5) were pre-incubated with agonist-mix (CpG-ODN+sCD40L+IL10) for 12h, as described in Supplementary Methods. Then cultures were added with pharmacologically relevant concentration of inhibitor of IKKα/β (BMS-345541, 12 μM) that blocks both classical and alternative NF-kB signaling[1]. One hour after addition of drugs, a second dose of agonist mix was added for an additional 12h. The expression of anti-apoptotic proteins Mcl-1, Bcl-xL, and Bcl-2 was analyzed in viability dye negative (live) CLL (CD5^{+}/CD19^{+}) cells by FCM. (**B-D)** CLL patient PBMCs (N=5) were pre-incubated with agonist-mix for 12h, as described in panel A. Then cells were incubated with pharmacologically relevant concentrations of inhibitor of IRAK4 [CA-4948, 10 μM; Compound 26[2], 0.5 μM], p38 (BIRB796, 5 μM)[3] , NIK (TRC694, 160 nM), pan-PI3K (GDC941, 1.248 μM)[4,5], or Btk (ibrutinib, 0.2 μM)[1] for 1h and a second dose of agonist-mix was added for an additional 12h as in Panel A. The target inhibition for CA-4948 and TRC694 was determined by FCM analysis of p-IRAK4 in IL-1β treated KARPASS-266 cells and ImageStream analysis of p100/52 nuclear localization in Z-138 MCL cell line that shows constitutively active alternative NF-kB signaling, respectively (data not

shown). (B) Expression of anti-apoptotic proteins Mcl-1, (C) Bcl-xL, and (D) Bcl-2 was analyzed by FCM as described in Panel A. Statistical significance was determined by ANOVA with Sidak's post-hoc test for multiple comparisons. *p<0.05, **p<0.01, ***p<0.001, ns- not significant. Data is presented as mean ± SD.

Supplementary Figure 5. CLL cell with activation phenotype *in vivo* exhibit resistance to BH-domain antagonists as well as BH-domain antagonist and ibrutinib combinations. (A-B) Freshly frozen PBMCs from various CLL patients (Pt 08, 27, 52, 70, and 95) were screened using the apoptosis threshold assay (ATA) by incubating with inhibitor of Bcl-2, Mcl-1, or Bcl-xL for 3h without added agonists as described in Figure 3A-B. Percentage of $CD69^{Pos}$ or $CD69^{Neg}$ CLL cells positive for cleaved caspase-3 and cleaved PARP from multiple patient samples exposed to various pro-apoptotic agents in ATA. **(C)** Freshly frozen PBMCs from various CLL patients were screened in ATA by incubating with inhibitor of Bcl-2 (venetoclax/VEN- 12.5 nM), Mcl-1 (S63845/S63- 2.05 μM), or Bcl-xL (A1155463/A1155- 16 μM) with or without ibrutinib (IBR) (0.1 μM) for 3h without added agonists. Ibrutinib at 0.1 μM was able to completely inhibit BTK phosphorylation in CLL cells, which was determined in our previous study[1]. Data showing percentage $CD69^{Pos}$ or $CD69^{Neg}$ CLL cells positive for cleaved caspase-9 from multiple patient samples exposed to various drugs in apoptosis threshold assay. **(D)** CLL patient PBMCs were processed as in panel A. Data showing percentage $CD38^{Pos}$ or $CD38^{Neg}$ CLL cells positive for cleaved caspase-9 from multiple patient samples exposed to various drugs in apoptosis threshold assay. The data in panel A-D are presented after subtracting spontaneous apoptosis values from DMSO treatment controls. **(E)** The CD69, CD38, and CD49d expression was analyzed in various CLL patient PBMCs using FCM. Data showing percentage $CD38^{Pos/Neg}$ or $CD49d^{Pos/Neg}$ CLL cells expressing CD69. Statistical significance was determined by ANOVA with Sidak's post-hoc test for multiple comparisons. *p<0.05, **p<0.01, ***p<0.001, ns- not significant. Data is presented as mean ± SD.

Supplementary Figure 6. Persister cells in venetoclax treated CLL patients are enriched for leukemic B-cells displaying functional and molecular profile of anti-apoptotic multi-drug resistance. (A) Anti-apoptotic proteins expression was analyzed by FCM in CLL (viability $dye^{Neg}/CD5^{+}/CD19^{+}$) cells in patient PBMCs (N=5) taken prior to or during treatment with

venetoclax as shown in Figure 4A. Data is presented as fold difference in GMFLI of pre versus during venetoclax treatment. **(B)** The percentile fluorescence intensity of individual anti-apoptotic proteins (Mcl-1, Bcl-xL, and Bcl-2) for each cell were classified into high (66-100%), medium (33-66%), and low (0-33%) expression classes and visualized as percent stacked bar charts for each patient. (**C)** FCM data showing percentage CLL cells positive for CD69, Ki67**,** and CXCR4 in patient PBMCs (N=5) taken prior to or during treatment with venetoclax, as shown in Panel A. Data is presented as mean ± SD.

Supplementary Figure 7. Inhibition of multiple anti-apoptotic proteins simultaneously resensitizes multi-drug resistant CLL cells, but this approach shows significant toxicity in healthy lymphocytes in patient PBMCs. (A) CLL patient PBMCs (N=16) were treated with inhibitor of Bcl-2 (venetoclax, 50 nM), Mcl-1 (S63845, 273 nM), and Bcl-xL (A1155463, 16 μM) (singly or in combination) for 9h. Cleaved PARP was analyzed in $CD69^{Pos}$ or $CD69^{Neg}$ CLL **(**$CD5^{+}$/$CD19^{+}$**)** cells by FCM. (**B)** CLL patient PBMCs (N=11) were processed as in panel A. The CD5+ healthy lymphocytes were identified using FCM as shown in left panel. Cleaved PARP in CD5+ healthy lymphocytes was analyzed by FCM (right panel). The data in panel A-B is presented after subtracting spontaneous apoptosis values form DMSO treatment controls. Statistical significance was determined by ANOVA with Sidak's post-hoc test for multiple comparisons. **p<0.01, ***p<0.001, ****p<0.0001, ns- not significant. Data is presented as mean ± SD.

Supplementary Figure 8. Venetoclax combination with chemotherapy agents overcome multi-drug resistance in CLL cells, but these combinations are moderately toxic to normal T lymphocytes. (A-B) CLL patient PBMCs were pre-incubated with the combination of CpG-ODN, sCD40L, and IL10 ("agonist-mix") for 12h. Then, samples were treated with venetoclax (25 nM) in combination with increasing concentrations of chemotherapy agents bendamustine (6.87, 13.74, 27.48, 54.9 μM), vincristine (3.13, 12.5, 50, 100 nM), or fludarabine (104, 208, 416, 836 μM) as well as second dose of agonist mix for 24h. Agonist-mix treatment has been shown to induce multi-drug resistance phenotype in CLL cells *ex vivo* (data not shown). (A) The cleaved PARP in $CD5^{+}$/$CD19^{+}$ (CLL) cells was analyzed by FCM. (B) Bar graphs showing Bliss predicted and actual (i.e., observed) cytotoxicity for the combination of

venetoclax (25 nM) with bendamustine (54.9 μM), vincristine (100 nM), or fludarabine (836 μM). (**C)** The cleaved PARP in $CD3^+/CD5^+$ cells (normal T lymphocytes) was analyzed by FCM. The data in panel A and C is presented after subtracting spontaneous apoptosis values from DMSO treatment controls. Statistical significance was determined by ANOVA with Sidak's post-hoc test for multiple comparisons. *p<0.05, **p<0.01, ***p<0.001. Data is presented as mean ± SD.

Supplementary Figure 9. Venetoclax drug combinations are ineffective in Bax/Bak double knockout CLL cells. (A) Bax and Bak double knockout CLL cell line (MEC1) was developed using CRISPR/Cas9 system, as described in the Supplementary Methods. Western blot data showing expression of Bax and Bak proteins in wild type and Bax/Bak double knockout (DKO) clones (left panel). **(B-D)** The wild type and Bax/Bak DKO cells were treated with DMSO, venetoclax (25 nM) or venetoclax with various partner drugs MNL4924 (1 μM), bortezomib (8 nM), or MI-2 (1.5 μM) for 18h. The apoptosis induction was determined by analyzing cleaved PARP using flow cytometry. The average data from two independent experiments presented as bar graph showing percentage MEC1 cells positive for cleaved PARP. Data is presented as mean ± SD.

Supplementary Figure 10. Targeting Mcl-1 in combination with agents that decrease apoptosis threshold overcome multi-drug resistance in CLL cells. (A-D) CLL patient PBMC were pre-incubated with agonist-mix for 12h. Then, samples were treated with Mcl-1 inhibitor S63845 (210 nM) in combination with BMS345541 (2, 4, 6, 8 μM), MI-2 (0.18, 0.37, 0.75, 1.5 μM), bortezomib (1, 2, 4, 8 nM), or pevonedistat/MLN4924 (0.25, 0.5, 0.75, 1 μM) or chemotherapy agents bendamustine (6.87, 13.74, 27.48, 54.9 μM), vincristine (3.13, 12.5, 50, 100 nM), or fludarabine (104, 208, 416, 836 μM) as well as second dose of agonist-mix for 24h. The cleaved PARP in $CD5^+/CD19^+$ (CLL) cells was analyzed by FCM (A-B). The cleaved PARP in $CD3^+/CD5^+$ cells (normal T lymphocytes) was analyzed by FCM (C-D). The data in panel A-D are presented after subtracting spontaneous apoptosis values from DMSO treatment controls. Statistical significance was determined by ANOVA with Sidak's post-hoc test for multiple comparisons. *p<0.05, **p<0.01, ***p<0.001, ns- not significant. Data is presented as mean ± SD.

Supplementary Figure 11. CLL cells activated by incubation with agonist-mix *ex vivo* exhibit pH2A.X expression following treatment with bendamustine or fludarabine. (A-C) CLL patient PBMCs were pre-incubated with the combination of CpG-ODN, sCD40L, and IL10 ("agonist-mix") or mock for 12h and treated with bendamustine (13.75, 27.48, and 54.9 μM) or fludarabine (104, 208, and 416 μM) as well as second dose of agonist mix for 24h. Phospho-histone H2A.X expression was analyzed by FCM in live (viability dye negative) and non-apoptotic (cleaved PARP negative) CLL ($CD5^+/CD19^+$) cells. (A) FCM panels showing phospho-histone H2A.X in a representative CLL sample treated with bendamustine (54.9 μM) for 18h. Data showing percentage CLL cells positive for phospho-histone H2A.X expression in patient samples treated with bendamustine (B) or fludarabine (C). Statistical significance was determined by ANOVA with Sidak's post-hoc test for multiple comparisons. *p<0.05, **p<0.01, ***p<0.001, ****p<0.0001, ns- not significant. Data is presented as mean ± SD.

Supplementary Tables.

Supplementary Table 1. Antibodies and reagents used in the study.

Drugs/Antibodies/reagents	Source (Company)
CpG oligodeoxynucleotides 2006	InvivoGen, San Diego, CA, USA.
Recombinant human IL-10	PeproTech, Rocky Hill, NJ, USA.
7AAD	BD Biosciences, San Jose, CA, USA.
Soluble human CD40L	GenScript, Piscataway, NJ. USA.
Mouse IgG blocking antibody for FACS analysis	Fitzgerald Industries, Acton, MA, USA.
Antibodies: Anti-Bcl-xL (clone 54H6), anti-BAK (clone D4E4), anti-p65/RelA (clone D14E12), anti-RelB (clone C1E4), anti-p100,52 (clone 18D10), anti-p-p65 (S536) (clone 93H1), anti-p-AKT (S473) (clone 193H12), anti-p-p38 (T180/Y182) (clone D3F9), anti-p-IRAK4 (T345/S346) (clone D6D7), anti-	Cell Signaling Technologies, Danvers, MA, USA.

Mcl1 or anti-Mcl1-AF488 (clone D2W9E), anti-Bcl2 or anti-Bcl2-PE (clone 124), anti-BIM or anti-BIM-AF647 (clone C34C5), Anti-cleaved caspase-9 (Asp315) (clone D8I9E). Anti-phospho-Histone H2A.X (Ser139) (clone 20E3)	
Anti-rabbit (H+L)-AF488, Anti-rabbit (H+L)-AF594, and anti-CD38 APC-CY5.5 (clone HIT2)	Invitrogen, Eugene, OR, USA
Antibodies: Anti-CD3-PerCP/Cy5.5 (clone UCHT1), Anti-CD5-APC (clone UCHT2), anti-CD5-APC/CY7 (clone UCHT2), anti-CD5-BV786 (clone L17F12), anti-CD19-BV421 (clone HIB19), anti-CD69-PE/CF594 (clone FN50), anti-cleaved PARP-PE or FITC (clone F21-852), anti-RAN (clone 20/Ran), anti-CD49d-PE-CY5 (clone 9F10), and anti-cleaved caspase3-AF647 (clone C92-605)	BD Biosciences, San Jose, CA, USA.
Anti-CD69-BV605 (clone FN50), anti-CXCR4-PE/CY7 (clone 12G5), anti-BAX-AF488 (clone 2D2), anti-BAX (clone 2D2), and Ki67-BV711 (clone Ki67).	BioLegend, San Diego, CA, USA
Live/Dead viability stains (far infrared or Aqua)	Invitrogen, Eugene, OR, USA
eBioscience Perm/Wash buffer (10X)	Invitrogen, Eugene, OR, USA

Supplementary Table 2. Clinical characteristics and treatment history of CLL patients.

Pt. No.	Age	Gender	Diagnosis	Previous therapy	FISH studies	Experiments conducted
01	68	M	CLL	FR, ofatumumab	Del13q	Figure 1, 3, and S1B. Multi-drug resistant cell analysis with agonist mix (data not shown).
02	80	F	CLL	Never treated	Trisomy 12	Figure 1, 3, and S1B. Multi-drug resistant cell analysis with agonist mix (data not shown).
03	84	F	CLL	Chlorambucil	Del13q	Figure 1, 3, and S1B. Multi-drug resistant cell analysis with agonist mix (data not shown).
04	75	M	CLL	R-CVP, FR, BR, ofatumumab	Trisomy 12	Multi-drug resistant cell analysis with agonist mix (data not shown).
07	81	M	CLL	Never treated	Trisomy 12	Figure 1, 3, and S1B.
08	69	F	CLL	Never treated	Del13q	Figure 1, 3, and S1B. Multi-drug resistant cell analysis with agonist mix (data not shown).
25	68	M	CLL	Never treated	Del13q	Figure 1, 3, and S1B. Multi-drug resistant cell analysis with agonist mix (data not shown).
27	66	F	CLL	rituximab	Del13q	Figure 1, 3, and S1B. Multi-drug resistant cell analysis with agonist mix (data not shown).

28	80	M	CLL	Bendamustine, rituximab, CVP	Trisomy 12	Figure 1, 3, and S1B.
33	63	M	CLL	Obinutuzumab plus bendamustine	Complex	Figure 1, 3, and S1B. Multi-drug resistant cell analysis with agonist mix (data not shown).
35	-	F	CLL	Fludarabine, FCR	Trisomy 12	Figure 1 and S1B.
41	65	M	CLL	Bendamustine, rituximab	Del13q	Figure 1 and 3. Multi-drug resistant cell analysis with agonist mix (data not shown).
46	68	M	CLL	Bendamustine, rituximab, IBR	Complex including Del 17p	Figure 1 and S1B. Multi-drug resistant cell analysis with agonist mix (data not shown).
52	61	M	CLL	Never treated	Normal	Figure 1, 3, and S1B. Multi-drug resistant cell analysis with agonist mix (data not shown).
56	56	F	CLL	Never treated	Del13q	Figure 1, 3, and S1B.
64	61	F	CLL	FR, BR, IBR	Del13q, Del 17p	Figure 1, 3, and S1B. Multi-drug resistant cell analysis with agonist mix (data not shown).
70	77	F	CLL	Chlorambucil and obinutuzumab	Trisomy12, del17p	Figure 1, 3, and S1B.

75	48	F	CLL	Zanubrutinib	Del13q, Del17p	Figure 1, 3, and S1B. Multi-drug resistant cell analysis with agonist mix (data not shown).
80	79	F	CLL	Never treated	Normal	Figure 1, 3, and S1B.
81	81	M	CLL	Never treated	Del13q	Figure 1, 3, and S1B. Multi-drug resistant cell analysis with agonist mix (data not shown).
90	58	M	CLL	Never treated	N/A	Figure 1, 3, and S1B.
95	51	M	CLL	Never treated	Del11q	Figure 3.

Abbreviations: IBR, ibrutinib; BR, bendamustine and rituximab; FCR, fludarabine, cyclophosphamide and rituximab; FR, fludarabine and rituximab; N/A, not available.

Supplementary Table 3. Nuclear localization of RelA, RelB, p100,52 in fixed frozen samples of CLL patients.

Pt. No.	RelA Nuclear Localization (%)			RelB Nuclear Localization (%)			p100,52 Nuclear Localization (%)			RelA Nuclear Localization (fold difference)			RelB Nuclear Localization (fold difference)			p100,52 Nuclear Localization (fold difference)		
	A	B	C	A	B	C	A	B	C	A	B	C	A	B	C	A	B	C
3	-	-	-	5.6	13.2	18.9	7.4	13.4	20.5	-	-	-	1.0	2.4	3.4	1.0	1.8	2.8
7	20.3	29.8	26.7	2.1	3.8	4.5	3.1	4.6	5.7	1.0	1.5	1.3	1.0	1.8	2.1	1.0	1.5	1.8
8	12.3	25.2	28.0	2.7	5.0	3.4	3.7	3.1	3.1	1.0	2.1	2.3	1.0	1.9	1.3	1.0	0.8	0.9
27	24.5	52.4	57.3	12.0	11.6	14.2	5.2	4.9	17.0	1.0	2.1	2.3	1.0	1.0	1.2	1.0	0.9	3.2
33	33.3	46.2	64.5	67.1	77.5	75.3	30.2	32.6	34.8	1.0	1.4	1.9	1.0	1.2	1.1	1.0	1.1	1.2
64	12.3	10.8	24.5	7.3	6.8	7.4	2.7	2.7	4.5	1.0	0.9	2.0	1.0	0.9	1.0	1.0	1.0	1.7
70	34.9	63.2	44.8	1.3	1.4	3.2	2.0	1.7	3.0	1.0	1.8	1.3	1.0	1.1	2.5	1.0	0.9	1.5

75	6.0	9.3	14.0	-	-	-	19.4	29.2	31.2	1.0	1.6	2.4	-	-	-	1.0	1.5	1.6
90	5.1	8.0	10.3	11.6	17.4	22.4	23.8	32.3	34.0	1.0	1.6	2.0	1.0	1.5	1.9	1.0	1.4	1.4

Abbreviations: A, $CD5^{+}/CD19^{+}/CD69^{-}/CXCR4^{High}$; **B,** $CD5^{+}/CD19^{+}/CD69^{+}/CXCR4^{High}$; **C,** $CD5^{+}/CD19^{+}/CD69^{+}/CXCR4^{Low}$. Fold difference was calculated by comparing nuclear localization values (RelA, RelB, p100,52) in $CD5^{+}/CD19^{+}/CD69^{+}/CXCR4^{High}$ or $CD5^{+}/CD19^{+}/CD69^{+}/CXCR4^{Low}$ with $CD5^{+}/CD19^{+}/CD69^{-}/CXCR4^{High}$.

Supplementary Table 4. Clinical characteristics and treatment history of CLL patients treated with venetoclax.

Patient No.	FISH studies	Circulating CLL ($CD5^{+}/CD19^{+}$) cells (%)		Absolute lymphocyte count (per μl)		Treatment history prior to VEN therapy	Clinical response to VEN treatment
		Pre VEN	During VEN	Pre VEN	During VEN		
12	Del13q	92.2	35.0	47290	5580	BR, Ofatumumab, CP, IBR	CR
21	Del11q, Trisomy 12	40.8	2.1	1580	2310	IBR	CRi
29	Del17p, Trisomy 12	5.2	1.5	1020	1020	Fludarabine, CP, R-CVP, Ofatumumab, IBR, Rituximab	CRi
31	N/A	9.67	1.31	1880	1020	Rituximab, CP, Obinutuzumab, IBR,	CR
71	Del17p	57.2	43.4	56890	27990#	IBR	CR
71	Del17p	57.2	43.4	56890	6590##	IBR	CR

Abbreviations: VEN, venetoclax; IBR, ibrutinib; BR, bendamustine and rituximab; CP, chlorambucil and prednisone; R-CVP, rituximab, cyclophosphamide, vincristine, and

prednisone; CR, complete response; CRi, complete response with incomplete marrow recovery. Clinical response to venetoclax treatment was assessed based on the criteria set by the International Workshop on Chronic Lymphocytic Leukemia (iwCLL)[6]. #, 3 days of venetoclax treatment. ##, 27 days of venetoclax treatment.

Supplementary Table 5. Table showing cluster information for every CLL patient samples taken prior to and during treatment of venetoclax.

Pt. No.	Pre-venetoclax treatment samples										During venetoclax treatment samples									
	CL1	CL2	CL3	CL4	CL5	CL6	CL7	CL8	CL9	CL10	CL1	CL2	CL3	CL4	CL5	CL6	CL7	CL8	CL9	CL10
12	19%	3%	16%	5%	1%	2%	4%	22%	5%	23%	19%	2%	10%	5%	2%	2%	3%	23%	7%	27%
21	38%	5%	11%	6%	3%	2%	5%	10%	4%	16%	25%	5%	31%	8%	3%	5%	8%	3%	2%	10%
29	29%	7%	28%	6%	2%	3%	11%	2%	3%	10%	2%	0%	3%	0%	1%	2%	4%	29%	7%	52%
31	34%	5%	15%	5%	3%	2%	3%	8%	5%	20%	0%	0%	0%	3%	0%	0%	0%	17%	11%	69%
71	32%	7%	22%	5%	2%	3%	3%	5%	2%	19%	8%	1%	5%	4%	1%	1%	2%	38%	10%	30%
AVR	30%	5%	18%	5%	2%	2%	5%	9%	4%	18%	11%	2%	10%	4%	1%	2%	3%	22%	7%	38%

Supplementary Table 6. Anchor and partner drugs used in the combination drug screen performed in an *ex vivo* microenvironmental model.

Anchor drug		Partner drug	
Drug name	**Target**	**Drug name**	**Target**
Venetoclax#	Bcl-2	Fludarabine#	DNA
S63845†	Mcl-1	Bendamustine#	DNA
		Vincristine#	Microtubule
		Pevonedistat/ MLN4924#	NEDD8-activating enzyme (NAE)
		Bortezomib#	proteasome
		MI-2†	MALT1

#, Already FDA approved, used in leukemia/lymphoma patients, or tested in clinical trials in human patients. **†**, Tool compound or under clinical development.

Supplementary Materials and Methods.

Drugs, reagents, and patient samples. IRAK4 inhibitor CA-4948 and NIK inhibitor TRC-694 were obtained from Curis, Inc and TRACON Pharmaceuticals, Inc, respectively. Details of other reagents are included in Table S1.

Peripheral Blood Mononuclear Cells (PBMC) collection, processing, and drug treatment. After local institutional review board approval and in accordance with the Declaration of Helsinki, informed consent was obtained from all CLL patients. Whole blood was collected and processed into PBMC by Ficoll density gradient centrifugation at the Biorepository and Tissue Research Facility (BTRF), the University of Virginia. PBMC samples were used as fresh or frozen in 90% fetal calf serum and 10% DMSO. Frozen samples were maintained in liquid nitrogen until further use. Patient samples were cultured in HEPES/Pyruvate supplemented RPMI containing 10% fetal calf serum. For *ex vivo* drug screening of patient samples (Fig. 5, S6-8), patient PBMC samples were cultured with or without agonists [CpG-ODN (1.5 μg/ml)+sCD40L (2 μg/ml)+IL-10 (15 ng/ml); "agonist-mix"]. Samples were treated with various inhibitors as well as a second dose of agonist mix as described earlier[1] and Legends. At the end of drug treatment, cells were subjected to downstream analysis.

NF-kB transcription factors nuclear localization analysis by imaging flow cytometry (ImageStream).

To assess RelA, RelB, and p100/52 nuclear localization in circulating CLL cells, we used fixed frozen whole blood (FFWB) samples for analysis of NF-kB nuclear localization, as we noticed that the NF-kB nuclear localization is highly sensitive to sample manipulation during PBMC isolation. FFWB were thawed at 4°C and RBCs were removed by washing with MojoSort Buffer (1xPBS, 0.5% BSA, and 2 mM EDTA). Then, samples were blocked with mouse immunoglobulin G (IgG) and stained for surface proteins CD5, CD19, CD69, and CXCR4 using CD5-APC, CD19-BV421, CD69-PE/CF594, and CXCR4-PE/CY7 antibodies for 1h at 4°C. Then, cells were permeabilized with saponin buffer (eBioscience, San Jose, CA) at 4°C for 20 min and stained for intracellular proteins RelA, RelB, or p100,52 with respective primary antibody followed by anti-rabbit-AF488 secondary antibody. The nucleus was stained using 7AAD. Details of antibodies used in imaging FCM analysis are included in Table S1. Imaging

FCM was carried out using an Amnis ImageStreamX Mark II imaging flow cytometer (Amnis Corporaton, Seattle WA) at the University of Virginia flow core facility. Imaging FCM data analysis was done using Image Data Exploration and Analysis software (IDEAS®), Amnis Corporation, WA.

Apoptotic protein staining for analytical flow cytometry. Apoptotic protein expression was analyzed by FCM as follows: Dead cells were stained using Live/Dead Aqua viability stain (Life Technologies, Grand Isle, NY) for 20 min at 4°C. Then, samples were fixed, blocked, stained for surface proteins CD5, CD19, CD69, and CXCR4 using anti-CD5-APC/CY7, CD19-BV421, CD69-BV605, and CXCR4-PE/CY7 respectively, and permeabilized with saponin as described above. The intracellular proteins Mcl-1, Bcl-2, Bim, and Bax were stained using anti-Mcl-1-AF488, anti-Bcl-2-PE, anti-Bim-AF647, and anti-BAX-AF488 (clone 2D2 that recognizes both active and inactive forms) antibodies, respectively. Bcl-xL, Bak (clone D4E4 that recognizes both active and inactive forms), and Puma were stained using respective primary antibodies followed by anti-rabbit-AF594 secondary antibody. Mcl-1, Bcl-2, Bim, and Bcl-xL were stained together in a panel along with surface markers, and all other apoptotic proteins were stained individually along with surface markers in separate tubes. Protein expression was assessed by calculating Geometric Mean Fluorescence Intensity (GMFLI). Apoptotic protein expression was analyzed in live cells by excluding Live/Dead Aqua positive cells. Details of antibodies are included in Table S1. FCM was performed using Attune NXT (Life Technologies) and CytoFLEX S (Beckman Coulter) analytical flow cytometers. FCM data analysis was done using FlowJo software (version 10.5.3) (Ashland, OR).

Phosphoprotein protein staining for analytical flow cytometry. Phosphoproteins in Figure S2 were analyzed by FCM as follows: PBMCs were isolated from unstimulated fresh whole blood samples in presence of Pervanadate and Calyculin A using SepMate™ PBMC Isolation Tubes (STEMCELL Technologies, MA) and immediately fixed in 1.6% paraformaldehyde (PFA) for 20 min at room temperature. Entire process of PBMC isolation using SepMate™ PBMC Isolation Tubes takes only 10-15 min, by following company's protocol. Cells were stained for surface markers CD5, CD19, CD69, and CXCR4 using anti-CD5-APC/CY7, anti-CD19-BV421, anti-CD69-BV605, and anti-CXCR4-PE/CY7 antibodies respectively.

Subsequently, cells were permeabilized in 50% methanol for 20 min at 4°C and stained for p-p65, p-AKT, p-p38, or p-IRAK4 primary antibodies for overnight followed by anti-rabbit-AF488 secondary antibody for 1h at 4°C. All these phosphoantibodies were tested in Western blot (WB) assays and validated for FCM using cells treated with agonists that activate respective kinases and/or target kinase inhibitors (data not shown). Phosphoprotein expression differences were determined by calculating GMFLI. Details of antibodies are included in Table S1.

The pH2A.X expression in Figure S9 was analyzed as follows: Samples were stained with Live/Dead Aqua viability stain (Life Technologies, Grand Isle, NY). Then, samples were then fixed, blocked, stained for surface markers CD5 and CD19 using anti-CD5-APC and anti-CD19-BV421 antibodies, respectively. Subsequently, cells were permeabilized in 50% methanol for 20 min at 4°C and stained for p-H2A.X primary antibodies for overnight followed by anti-rabbit-AF488 secondary antibody for 1h. Then, cells were stained for anti-cleaved PARP-PE. The pH2A.X expression was analyzed in live (viability dye negative) and non-apoptotic (cleaved PARP negative) CLL ($CD5^+/CD19^+$) cells. Protein expression differences were determined by calculating GMFLI. Details of antibodies used in analytical FCM analysis are included in Table S1.

FCM was performed using Attune NXT (Life Technologies) and CytoFLEX S (Beckman Coulter) analytical flow cytometers. FCM data analysis was done using FlowJo software (version 10.5.3) (Ashland, OR).

Drug induced cytotoxicity analysis by analytical flow cytometry. Dead cells were stained by incubating samples with Live/Dead near-infrared viability stain for 20 min at 4°C. Subsequently, samples were fixed in 1.6% PFA and blocked as described above. Then, surface proteins were stained by incubating with appropriate antibodies for 1h at 4°C. Intracellular proteins were stained with corresponding antibodies after permeabilizing cells with saponin based permeabilization buffer (eBiosciences, San Jose, CA) for 20 min at 4°C. Following antibody panel was used in Fig. S7A-B: Live/Dead near-infrared viability stain, anti-CD5-APC, anti-CD19-BV421, anti-CD69-BV605, and anti-cleaved PARP-FITC. In Fig. 5, S8, and S10: Live/Dead near-infrared viability stain, anti-CD5-APC, anti-CD19-BV421, anti-CD3-PerCP/CY5.5, anti-cleaved PARP-FITC. In Fig. S9: Live/Dead near-infrared viability stain and

PARP-PE. Antibody details are in Table S1. FCM was performed using Attune NXT (Life Technologies) and CytoFLEX S (Beckman Coulter) analytical flow cytometers. FCM data analysis was done using FlowJo software (version 10.5.3) (Ashland, OR).

Development of Bax and Bak double knockout CLL cell line MEC1. Bax and Bak double knockout MEC1 cell line was developed using CRISPR-Cas9 system. Multiple sgRNAs targeting human Bax and Bak1 genes were selected from the available Addgene CRISPR pooled sgRNA Library. Guide RNAs (gRNAs) targeting human BAX (CACCGTTTCTGACGGCAACTTCAAC; AAACGTTGAAGTTGCCGTCAGAAAC; CACCGA GTAGAAAAGGGCGACAACC; AAACGGTTGTCGCCCTTTTCTACTC) and BAK1 (CACCG ACGGCAGCTCGCCATCATCG; AAACCGATGATGGCGAGCTGCCGTC; CACCGTTGATG TCGTCCCCGATGA; AAACTCATCGGGGACGACATCAAC; CACCGCTCACCTGCTAGGTT GCAG; AAACCTGCAACCTAGCAG GTGAGC) were cloned into TLCV2 plasmid backbone (Addgene, #87360) using restriction enzyme BsmBI and confirmed by Sanger DNA sequencing. An empty TLCV2 was included as control. VSV pseudotyped lentiviruses expressing Bax and Bak sgRNAs and Cas9 and GFP proteins were generated by co-transfecting 293T cells with TLCV2 vectors containing pool of sgRNA targeting Bax/Bak and lentivirus packaging plasmids psPAX2 and pMD2. The transfection was performed using Lipofectamine 3000 transfection reagent (Thermo Fisher Scientific, USA). Lentiviruses were concentrated from the supernatants at 48h post-transfection through ultracentrifugation (125, 000*g* for 3h). The virus titer was determined by analyzing GFP expression in flow cytometry following transduction of Jurkat cells. MEC1 cells were transduced with 100 MOI of lentivirus expressing sgRNAs against Bax and Bak1 genes in presence of Polybrene. After 48h of transduction, cells were selected in presence of puromycin for a week. Subsequently, single cell clones were prepared by serial dilutions protocol and Bax/Bak expression loss was confirmed by Western blot. Doxycycline was added during puromycin selection as well as single cell cloning to induce Cas9 and GFP expression.

References.

1. Jayappa KD, Portell CA, Gordon VL, et al. Microenvironmental agonists generate de novo phenotypic resistance to combined ibrutinib plus venetoclax in CLL and MCL. *Blood Adv*. 2017;1(14):933–946.
2. Tumey LN, Boschelli DH, Bhagirath N, et al. Identification and optimization of indolo[2,3-c]quinoline inhibitors of IRAK4. *Bioorg Med Chem Lett*. 2014;24(9):2066–2072.
3. Jensen KJ, Garmaroudi FS, Zhang J, et al. An ERK–p38 subnetwork coordinates host cell apoptosis and necrosis during coxsackievirus B3 infection. *Cell Host Microbe*. 2013;13(1):67–76.
4. Liu X, Wang A, Liang X, et al. Characterization of selective and potent PI3Kδ inhibitor (PI3KDIN-015) for B-Cell malignances. *Oncotarget*. 2016;7(22):32641–32651.
5. Furcht CM, Buonato JM, Lazzara MJ. EGFR-activated Src family kinases maintain GAB1-SHP2 complexes distal from EGFR. *Sci Signal*. 2015;8(376):ra46.
6. Hallek M, Cheson BD, Catovsky D, et al. iwCLL guidelines for diagnosis, indications for treatment, response assessment, and supportive management of CLL. *Blood*. 2018;131(25):2745–2760.